ORIGINAL

# Early Prediction of Radiotherapeutic Efficacy in a Mouse Model of Non-Small Cell Lung Carcinoma Using $^{18}$F-FLT and $^{18}$F-FDG PET/CT

Tamaki Otani[1], Hitoshi Ikushima[2], Yoshimi Bando[3], Michiko Yamashita[4], Kenmei Kuwahara[5], Hideki Otsuka[6], Kazuya Kondo[7], and Hirokazu Miyoshi[1]

*[1]Advance Radiation Research, Education, and Management Center, Tokushima University, Tokushima, Japan, [2]Department of Therapeutic Radiology, Institute of Biomedical Science, Tokushima University, Tokushima, Japan, [3]Department of Pathology and Laboratory Medicine, Institute of Biomedical Science, Tokushima University, Tokushima, Japan, [4]Department of Analytical Pathology, Institute of Biomedical Science, Tokushima University, Tokushima, Japan, [5]Faculty of Health Science, Tokushima University Graduate School of Medicine, Tokushima University, Tokushima, Japan, [6]Department of Medical Imaging/Nuclear Medicine, Tokushima University Graduate School of Biomedical Sciences, Tokushima University, Tokushima, Japan, [7]Department of Oncological Medical Services, Institute of Biomedical Science, Tokushima University, Tokushima, Japan*

**Abstract : This study investigated the usefulness of [$^{18}$F]-3'-deoxy-3'-fluorothymidine ($^{18}$F-FLT) and [$^{18}$F]-fluoro-2-deoxy-D-glucose ($^{18}$F-FDG) positron emission tomography (PET)/computed tomography (CT) imaging for predicting the therapeutic efficacy of non-small cell lung cancer (NSCLC) irradiation at an early stage after radiation treatment. Mice were xenografted with the human lung adenocarcinoma line A549 or large cell lung cancer line FT821. Tumour uptake of $^{18}$F-FLT and $^{18}$F-FDG was imaged using PET/CT before and 1 week after irradiation. In A549 tumours, $^{18}$F-FLT uptake was significantly decreased, and $^{18}$F-FDG uptake was unchanged post-irradiation compared with pre-irradiation. In FT821 tumours, uptake of both $^{18}$F-FLT and $^{18}$F-FDG uptake was substantially decreased post-irradiation compared with pre-irradiation. In both xenografts, tumour volumes in the irradiated groups were significantly decreased compared with those in the control group. $^{18}$F-FLT is expected to contribute to individual NSCLC therapy because it accurately evaluates the decrease in tumour activity that cannot be captured by $^{18}$F-FDG. $^{18}$F-FDG may be useful for evaluating surviving cells without being affected by the inflammatory reaction at an extremely early stage, approximately 1 week after irradiation. Combined use of $^{18}$F-FLT and $^{18}$F-FDG PET/CT imaging may increase the accurate prediction of radiotherapy efficacy, which may lead to improved patient outcomes and minimally invasive personalised therapy. J. Med. Invest. 70 : 361-368, August, 2023**

***Keywords*** **:** *$^{18}$F-fluorodeoxyglucose, $^{18}$F-fluorothymidine, irradiation, inflammation, non-small cell lung cancer*

## INTRODUCTION

Several randomised controlled trials have investigated the usefulness of preoperative induction radiotherapy for non-small cell lung cancer (NSCLC), but no significant improvement in survival with neo-adjuvant chemoradiotherapy was confirmed (1, 2). Phase II trials of neo-adjuvant chemoradiation therapy for non-small cell lung cancer have reported variable response rates of 39% to 88% and complication rates of 0% to 67% (3-5). Thus, it is conceivable that the efficacy and side effects of treatment differ from case to case. In recent years, advances in testing technology have made it possible to provide individualised therapy that selects the optimal treatment method according to the patient's constitution. If the effect of neo-adjuvant chemoradiation therapy can be determined accurately, individualised treatment will be possible. This might include changing the treatment policy to radical chemoradiotherapy according to the treatment effect of each case, leading to improved treatment outcomes and a reduced burden on patients. Accurate diagnostic imaging by molecular imaging is essential for individualised cancer therapy. In this study, we demonstrated the usefulness of positron emission tomography/computed tomography (PET/CT) imaging to assess the effects of radiotherapy.

[$^{18}$F]-fluoro-2-deoxy-D-glucose ($^{18}$F-FDG) PET/CT is an excellent method for imaging tumours and the most commonly used imaging modality for accurately delineating tumour lesions (6, 7). However, when used to determine the effects of radiotherapy, infiltration of inflammatory cells around the tumour lesions, such as macrophages, may cause false positive results (8, 9). Inflammatory lesions present frequently at approximately 1 month after radiotherapy, and it is difficult to determine the efficacy of radiotherapy using $^{18}$F-FDG PET/CT at an earlier stage. [$^{18}$F]-3'-deoxy-3'-fluorothymidine ($^{18}$F-FLT) can be used to evaluate cell proliferation through the enzymatic activity of thymidine kinase 1. $^{18}$F-FLT is a tumour proliferation imaging tracer that is not affected by inflammation. Therefore, it is expected that $^{18}$F-FLT will be highly accurate for the evaluation of radiotherapy efficacy, even immediately after treatment (10, 11).

Owing to the inflammatory responses detected by $^{18}$F-FDG, many reports have evaluated the effects of radiotherapy approximately 4 months after treatment. However, few studies have determined or predicted the therapeutic effects within 1-month post-treatment. An early and precise diagnosis of lung cancer response is essential because surgery or re-irradiation with curative intent may be feasible. In this study, we investigated the usefulness of $^{18}$F-FLT and $^{18}$F-FDG PET/CT for determining the therapeutic efficacy of radiotherapy in NSCLC. We used mice

Received for publication October 26, 2022 ; accepted April 11, 2023.

Address correspondence and reprint requests to Tamaki Otani, Advance Radiation Research, Education, and Management Center, Tokushima University, 3-18-15 Kuramoto-cho, Tokushima 770-8503, Japan and Fax : +8188-633-9417. E-mail : otani.tamaki@tokushima-u.ac.jp

subcutaneously transplanted with human NSCLC cells to evaluate the effects of radiotherapy in the very early stage (1 week) after irradiation.

## MATERIALS AND METHODS

### *Animals*

Male nude mice (BALB/cAJcl-nu/nu ; CLEA Japan Inc. ; Tokyo, Japan) 6–8 weeks of age were used in this study and maintained in the Laboratory for Animal Experiments at our institution with a standardised 12-h light/dark cycle and access to food and water *ad libitum*. The protocols for all animal experiments were approved by and performed in accordance with the guidelines of the Institutional Animal Care and Use Committee of the University of Tokushima. The humanitarian endpoint for subcutaneously transplanted mice was euthanasia when the tumour diameter reached 20 mm.

### *Cell culture and transplantation*

We used two types of NSCLC cell lines : A549 (human adenocarcinoma lung cancer cells) and FT821 (human large cell lung cancer cells). We established the FT821 cell line using a primary culture from surgically resected tissue provided by Tokushima University (Tokushima, Japan) (12, 13). A549 cells were purchased from the Health Science Research Resources Bank (Osaka, Japan). The cell lines were cultured in RPMI 1640 (Sigma Chemical Co. ; St. Louis, MO, USA) supplemented with 10% heat-inactivated foetal bovine serum (BioWhittaker ; Walkersville, MD, USA) at 37°C in a humidified incubator equilibrated with 5% $CO_2$ and 95% air. Subcutaneous implantation of A549 or FT821 cells ($2.0 \times 10^6$/mouse) was performed in the lateral chest of the mice.

### *Irradiation*

Local external beam irradiation was applied using an X-ray irradiation unit (MBR-1520R-3 ; Hitachi ; Tokyo, Japan). A549 and FT821 were transplanted into mice, and the mice were divided into X-ray irradiation (20 Gy/2 fractions/2 days) and non-irradiation groups. Tumour irradiation was performed at 20 and 50 days after transplantation with A549 and FT821 cells, respectively. Areas other than the tumour were shielded with a lead barrier to prevent nonspecific radiation exposure.

### *$^{18}$F-FLT and $^{18}$F-FDG PET/CT measurements*

$^{18}$F-FLT and $^{18}$F-FDG PET/CT measurements were taken from mice in the control group prior to radiation treatment of the irradiation group, and from the irradiation group 1 week after radiation treatment (Fig. 1). Fourteen mice transplanted with A549 (control group : 7, irradiation group : 7) and 10 mice transplanted with FT821 (control group : 5, irradiation group : 5) were used for $^{18}$F-FLT and $^{18}$F-FDG PET/CT measurements. All scans were performed with a Siemens Inveon small-animal PET scanner (Siemens Healthcare ; Knoxville, TN, USA). Mice monitored by $^{18}$F-FDG PET/CT were fasted for 18–24 h with access to water only. Mice used for $^{18}$F-FLT PET/CT were not fasted. Body weights were measured, and mice were anaesthetised by 1.5%–2.0% isoflurane inhalation and injected via a tail-vein catheter with 10 MBq/0.1–0.2 mL $^{18}$F-FLT or $^{18}$F-FDG. The entire mouse body was scanned by CT and PET (field of view : 99.0

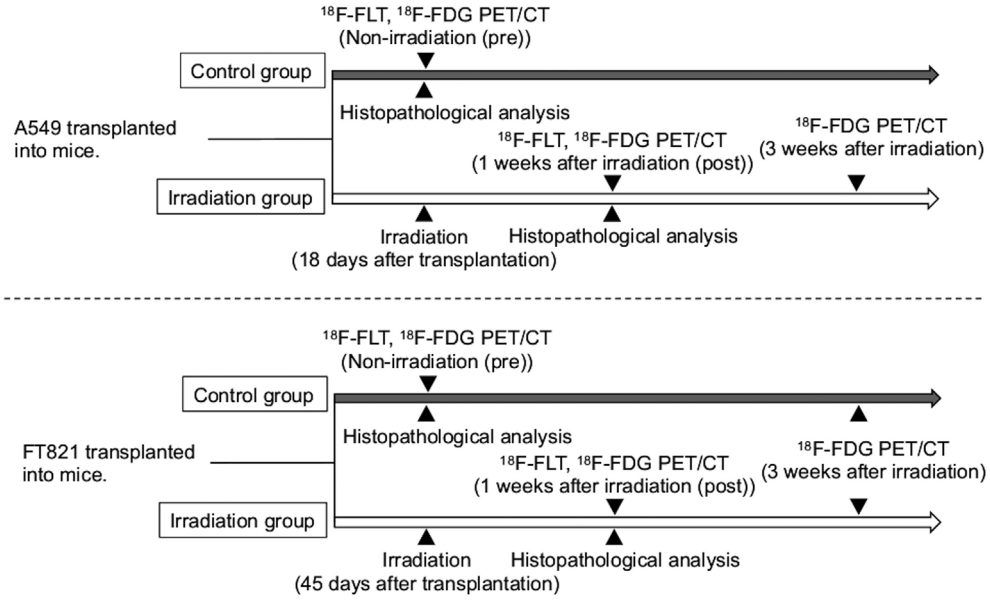


Fig 1. Schematic presentation of the study time course.
Non-small cell lung cancer cell lines A549 and FT821 were transplanted into mice, and the mice were divided into irradiation and control (non-irradiation) groups. [$^{18}$F]-3'-deoxy-3'-fluorothymidine ($^{18}$F-FLT) and [$^{18}$F]-fluoro-2-deoxy-D-glucose ($^{18}$F-FDG) positron emission tomography/computed tomography (PET/CT) measurements were performed on mice in the control group prior to radiation treatment of the irradiation group. $^{18}$F-FLT and $^{18}$F-FDG PET/CT measurements were performed on mice in the irradiation group 1 week after radiation treatment. Irradiation was performed at 18 and 45 days after transplantation of A549 and FT821 tumours, respectively. The same mice could not be evaluated using PET/CT pre- and post-irradiation because their removal from the PET/CT facility was prohibited to prevent radioactive contamination. Therefore, non-irradiation in the control group was defined as pre-irradiation (0 week), and 1 week after irradiation in the irradiated group was defined as post-irradiation for comparisons between the groups. At 3 weeks after irradiation, $^{18}$F-FDG PET/CT measurements were performed on the control and irradiation groups. There was no data for $^{18}$F-FDG PET/CT imaging of A549 tumours in the control group at 3 weeks because mice in the control group reached a humane endpoint regarding tumour size within 3 weeks and were sacrificed.

× 99.0 × 126.2 mm). PET data were acquired in list mode for 20 min following a delay of 40 min to allow for $^{18}$F-FLT and $^{18}$F-FDG uptake. PET images were reconstructed using three-dimensional ordered-subject expectation maximisation followed by maximum a posteriori reconstruction The image matrix was 128 × 128 pixels, and the slice thickness of the PET images was 0.796 mm. Only the $^{18}$F-FDG PET/CT measurement was performed again 3 weeks after irradiation.

*PET image analysis*

The PET/CT images were analysed using PMOD software (version 4.201 ; PMOD Technologies LLC. ; Zürich, Switzerland). The window levels of all PET images were displayed at 0–3 based on the standardised uptake value (SUV). For all PET/CT datasets, the volume of interest was defined manually around the area of $^{18}$F-FLT or $^{18}$F-FDG uptake by the tumour. Measurements included the maximum SUV ($SUV_{max}$), the averaged SUV ($SUV_{mean}$), and the metabolic tumour volume (MTV). The total lesion glycolysis (TLG) was the product of MTV and $SUV_{mean}$ (total lesion proliferation [TLP] was used for $^{18}$F-FLT imaging). The MTV and TLG (TLP), which reflect changes in tumour size, were recently used as indices of whole tumour uptake and might be useful for evaluate the therapeutic effect of radiotherapy more accurately. The clinical usefulness of these indicators for prognosis and treatment response was demonstrated in many cancers, including lung, head-and-neck, and gynaecological cancer (14, 15).

*Measurement of tumour volumes*

The major and minor axes of the tumours were measured for 3 weeks after irradiation using a calliper. Tumour volume was determined by the formula : $T_{vol} = \frac{Major\ axis \times (Minor\ axis)^2}{2}$.

*Histological examination*

Cell division, vascularisation, and radiation-induced inflammation were examined histologically by measuring levels of the cell proliferation marker Ki67 and number of viable neutrophils. Mice were sacrificed, and tumour specimens were removed at the same time point as PET/CT measurements in the control and irradiation groups 1 week after irradiation and resected *en bloc*. Each tumour was fixed in 10% phosphate-buffered formalin for 24–48 h, embedded in paraffin blocks, and processed for histological analysis. Sections were stained with haematoxylin and eosin or immunohistochemically using standard protocols. Briefly, tissue sections were heated in a pressure cooker in Tris-EDTA buffer for antigen retrieval. The sections were blocked using goat serum in phosphate-buffered saline followed by incubation with anti-Ki67 antibody (rabbit, clone SP6 ; Nichirei Bioscience Inc. ; Tokyo, Japan). Then, the sections were incubated with a biotinylated secondary antibody (Nichirei Bioscience, cat. #424031) and streptavidin-horseradish peroxidase followed by colorimetric detection using 3,3'-diaminobenzidine. Histology slides were observed under light microscopy at ×400 (high-power-field with a 0.2376 mm$^2$ field of view), and the Ki67 labelling index was quantified using the hot spot method (16). Viable neutrophils were counted within eight high-power fields at the surface and central area of each section. It was not possible to perform a pathological examination of mice that were subjected to PET/CT because their removal from the PET/CT facility was prohibited to prevent radiation exposure and/or radioactive contamination. Therefore, mice were prepared for pathological analysis separately from the mice used for PET. Fifteen (control group : 7, irradiation group : 8) and 18 (control : 10, irradiation : 8) mice xenografted with A549 and FT821 cells, respectively, were used for pathological analysis.

*Statistical analysis*

The quantitative values in the control-irradiation groups were compared using the Mann-Whitney *U*-test (SPSS software, version 20 ; IBM Corp. ; Armonk, NY, USA). Comparisons of quantitative values between 1- and 3-week irradiation groups were performed using the Wilcoxon signed rank test. A *p*-value of $< 0.05$ was considered statistically significant.

## RESULTS

*Prediction of the radiotherapeutic effect using $^{18}$F-FLT and $^{18}$F-FDG PET / CT*

Figure 2 shows representative $^{18}$F-FLT and $^{18}$F-FDG PET images from control (pre-irradiation) and irradiation (post-irradiation) groups. A marked decrease in A549 tumour uptake was observed visually with $^{18}$F-FLT imaging after irradiation compared with that in the control group. Figure 3 shows the quantitative indexes obtained from $^{18}$F-FLT and $^{18}$F-FDG PET/CT scans of mice in the control (pre) and irradiation (post) groups. A significant decrease in the $SUV_{max}$ was observed in the A549 tumours imaged with $^{18}$F-FLT after irradiation compared with those in the control (pre) group, but there was no change in FT821 tumours. In A549 tumours, the MTV and TLP were decreased in the irradiation (post) group only with $^{18}$F-FLT imaging compared with those in the control (pre) group. In FT821 tumours, the MTV and TLG (TLP) were decreased in the irradiation (post) group compared with those in the control (pre) group after $^{18}$F-FLT and $^{18}$F-FDG imaging.

*Evaluation of the therapeutic effect using tumour volume measurements*

The A549 tumour volumes in the irradiated group were significantly decreased compared with those in the control group ; however, the volumes appeared to increase gradually (Fig. 4a). The FT821 tumour volumes in the irradiated group of mice were significantly decreased compared with those in the control group, and there was no tendency towards an increase over time (Fig. 4b). For the A549 tumours, mice in the control group reached a humane endpoint in tumour size within 3 weeks and were sacrificed (Fig. 4c) survival curves). No mice died in the FT821 group.

*Evaluation of the therapeutic effect using $^{18}$F-FDG PET / CT*

Table 1 shows the quantitative indexes obtained from $^{18}$F-FDG PET/CT at 3 weeks after irradiation. No changes in the SUVs were observed in A549 tumours at the 1- and 3-week time points after irradiation ; however, the MTV and TLG were increased at 3 weeks compared with 1 week after irradiation. In FT821 tumours, a significant increase in the SUV, MTV, and TLG was observed in the control group at 3 weeks after irradiation compared with pre-irradiation, but no significant changes were observed within the irradiation group between 1 and 3 weeks after irradiation. In FT821 tumours, comparisons of values between the control and irradiation groups at the 3-week time point showed that the irradiation group had significantly lower SUV, MTV, and TLG.

*Evaluation of the therapeutic effect using histopathological analysis*

Figure 5 shows the haematoxylin-eosin staining of tumour tissues and Table 2 shows the percentage of Ki67+ cells and numbers of viable neutrophils 1-week post-irradiation. In the A549 and FT821 xenografts, necrotic lesions and degenerative tumour tissue were more common in the irradiated group than in the control group. Ki67 staining was significantly decreased

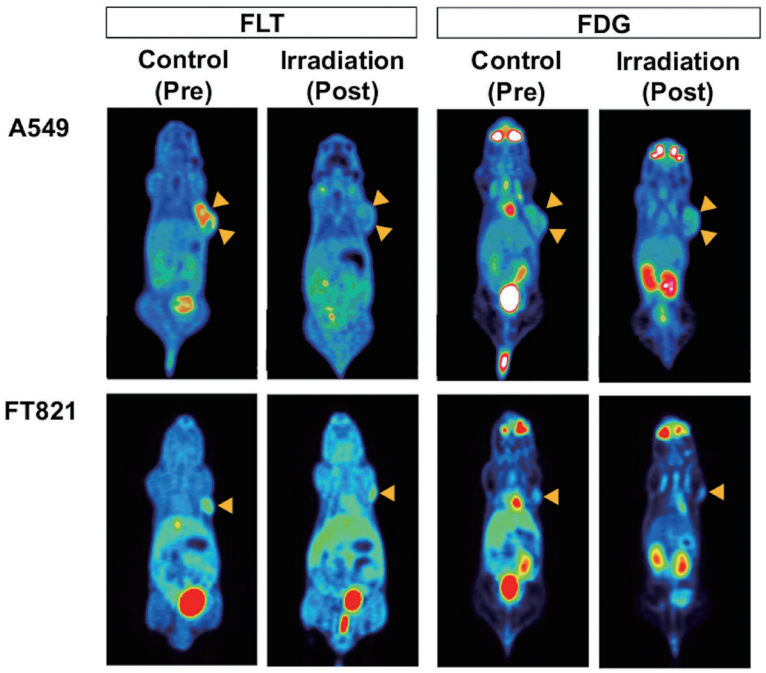


Fig 2. $^{18}$F-FLT and $^{18}$F-FDG PET images of mice.
Representative $^{18}$F-FLT and $^{18}$F-FDG PET images of mice in the control (pre-irradiation) and irradiation (post-irradiation) groups. The yellow arrows show $^{18}$F-FLT and $^{18}$F-FDG uptake by the xenografted tumours. All images were displayed with a window level of 0 to 3 based on standardised uptake volume.

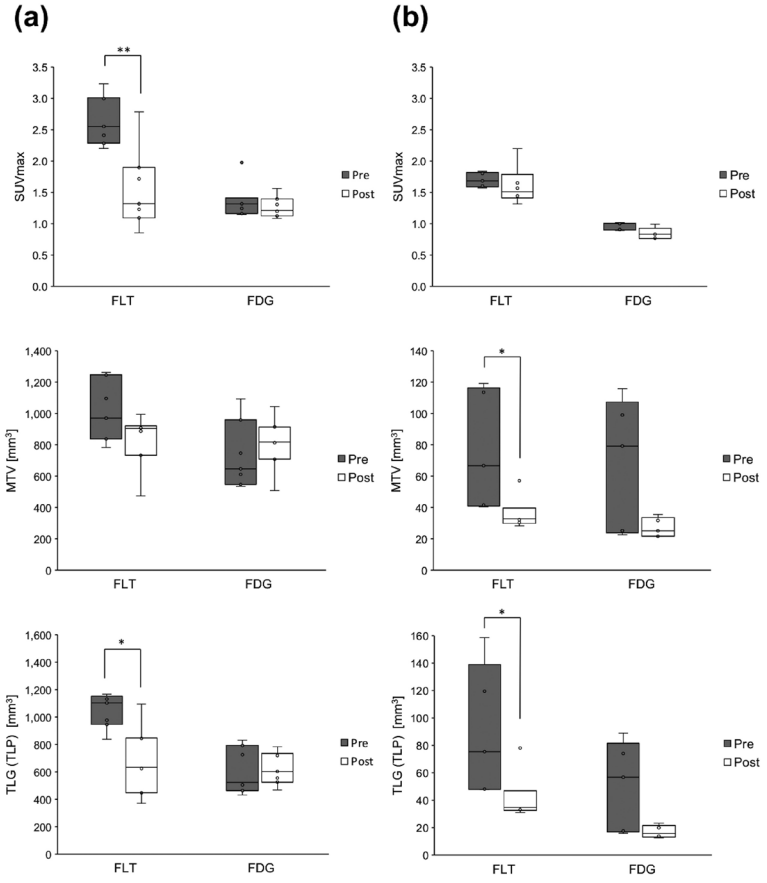


Fig 3. Quantitative indexes measured using PET/CT.
The maximum standardised uptake value ($SUV_{max}$), the metabolic tumour volume (MTV), and the total lesion glycolysis (TLG) of the control (pre) and irradiation (post) groups were measured using $^{18}$F-FLT and $^{18}$F-FDG PET/CT. (a) A549 and (b) FT821 tumours. The horizontal bar in the boxplot indicates the median. Comparisons of the quantitative indexes between control (pre) and irradiation (post) groups were performed using the Mann-Whitney *U*-test. *: $p < 0.05$, **: $p < 0.01$.

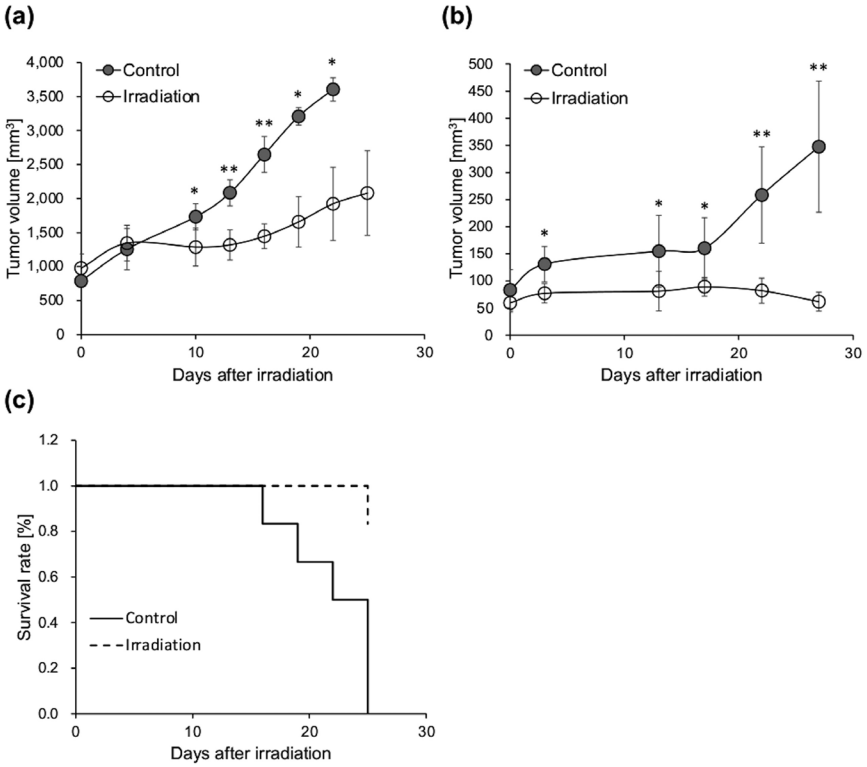


Fig 4. Change in tumour volumes.
Tumour volumes of xenografted tissue in control and irradiation groups. (a) A549 and (b) FT821 tumours. (c) In A549, mice in the control group reached a humane endpoint in tumour size within 3 weeks and were sacrificed, and the results are shown as survival curves. Comparisons of tumour volumes between control and irradiation groups were performed using the Mann-Whitney *U*-test. *: $p < 0.05$, **: $p < 0.01$.

Table 1. Quantitative indexes obtained from $^{18}$F-FDG PET/CT before and at 1 and 3 weeks after irradiation

| | A549 | | | FT821 | | | | |
|---|---|---|---|---|---|---|---|---|
| | Control | Post-irradiation | | Control | | Post-irradiation | | Comparisons of quantitative values between control and irradiated FT821 tumours at 3 weeks |
| | 0 week | 1 week | 3 weeks | 0 week | 3 weeks | 1 week | 3 weeks | |
| $SUV_{max}$ | 1.37 ± 0.28 | 1.27 ± 0.17 | 1.27 ± 0.13 | 0.96 ± 0.06 | 1.62 ± 0.23 | 0.84 ± 0.09 | 0.80 ± 0.11 | $p < 0.01$ |
| $SUV_{mean}$ | 0.84 ± 0.10 | 0.79 ± 0.14 | 0.82 ± 0.08 | 0.73 ± 0.03 | 0.97 ± 0.09 | 0.63 ± 0.07 | 0.66 ± 0.06 | $p < 0.01$ |
| MTV ($mm^3$) | 734.7 ± 214.8 | 805.3 ± 166.9 | 1051.8 ± 433.5* | 68.4 ± 42.6 | 393.5 ± 116.5 | 27.2 ± 6.3 | 16.9 ± 9.1 | $p < 0.01$ |
| TLG ($mm^3$) | 611.4 ± 167.1 | 628.0 ± 119.6 | 870.4 ± 424.6* | 50.7 ± 33.0 | 384.8 ± 126.8 | 17.1 ± 4.5 | 11.5 ± 7.1 | $p < 0.01$ |

*Comparisons of quantitative values between 1- and 3-week post-irradiation groups were performed using the Wilcoxon signed rank test ($p < 0.05$).
$^{18}$F-FDG, [$^{18}$F]-fluoro-2-deoxy-D-glucose ; PET/CT, positron emission tomography/computed tomography ; MTV, metabolic tumour volume ; SUV, standardised uptake value ; TLG, total lesion glycolysis.

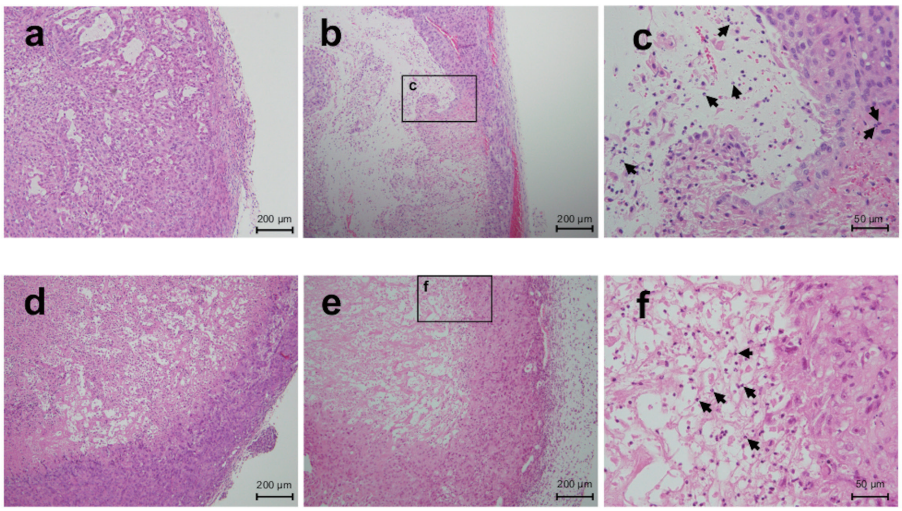


Fig 5. Histological sections of tumour tissue.
Representative haematoxylin and eosin-stained histological sections from A549 (a–c) and FT821 (d–f) tumours. Tumour tissues from the control (a, d) and irradiation (b, e) groups are shown at ×100 magnification. The square indicates the area with viable neutrophils that were confirmed at the margin of the necrotic lesions. This area is shown at ×400 magnification (c, f), and the arrows indicate the viable neutrophils.

Table 2. Histopathological results from A549 and FT821 tumour xenografts at 1 week after irradiation

| | | Control | Irradiation | *p* value* |
|---|---|---|---|---|
| A549 | Ki67 (%) | 60.5 ± 16.4 | 31.6 ± 5.2 | 0.05 |
| | Viable Neutrophil Number | 17.0 ± 4.9 | 20.8 ± 9.9 | 0.69 |
| FT821 | Ki67 (%) | 48.9 ± 11.5 | 23.3 ± 6.5 | 0.02 |
| | Viable Neutrophil Number | 20.5 ± 17.2 | 43.8 ± 34.9 | 0.12 |

*Comparisons of quantitative values between control and irradiation groups were performed using the Mann-Whitney *U*-test.

in the irradiated group compared with that in the control group for the A549 and FT82 xenografts. The number of viable neutrophils was used to assess the inflammatory response caused by irradiation. Viable neutrophils were confirmed at the margin of the necrotic lesions 1 week after irradiation (Fig. 5b and d) ; however, there were no significant changes in viable neutrophil numbers between the control and irradiation groups.

## DISCUSSION

As a result of the multifaceted evaluation of the therapeutic effects of irradiation using tumour volume measurements, $^{18}$F-FDG PET/CT, and pathological analysis, multiple anticancer effects were observed, which included a decrease in tumour volume, $^{18}$F-FDG uptake, and Ki67 index, and an increase in radiation-induced necrotic tumour regions. From these results, we concluded that a therapeutic effect of irradiation was obtained for the A549 and FT821 xenografts. However, in the A549 tumours, the tumour volume appeared to increase over time ; therefore, the tumour suppressive effect of irradiation may have been temporary. In view of these therapeutic effects, $^{18}$F-FLT and $^{18}$F-FDG PET/CT were analysed for their ability to predict radiotherapy efficacy.

When the therapeutic effects of radiotherapy using PET were investigated, the results differed depending on the quantitative indexes SUV, MTV, and TLG. In FT821 tumours, the MTV and TLG were more consistently altered than the SUV. Therefore, the MTV and TLG, which reflect changes in tumour size, can be used to evaluate the therapeutic effect of radiotherapy more accurately than the SUV. The usefulness of MTV and TLG was shown in previous studies (15, 16). The tumour volumes of the FT821 xenografts were small ; therefore, the $SUV_{max}$ may not have been measured accurately because of the influence of the partial volume effect (17).

Considering the $SUV_{max}$ as well as the MTV and TLG (TLP), $^{18}$F-FLT PET/CT showed a significant decrease in A549 and FT821 tumour uptake. Staining of Ki67, a histological index of tumour activity, was significantly decreased in the irradiated group compared with that in the control group for the A549 and FT821 xenografts. Previous studies reported that $^{18}$F-FLT uptake correlated with Ki67 levels (18, 21), and changes in $^{18}$F-FLT uptake reflected tumour activity, which is useful for judging therapeutic effects. The usefulness of $^{18}$F-FLT PET/CT for predicting therapeutic effects has been proposed in many studies, and the uptake of $^{18}$F-FLT may be better than $^{18}$F-FDG for predicting the radiotherapeutic response of tumours (18-24).

FT821 tumours, in which the $^{18}$F-FLT and $^{18}$F-FDG uptake

were decreased 1 week after treatment, underwent a significant antitumor effect, which was present even 3 weeks after treatment. However, in A549 tumours, $^{18}$F-FLT PET/CT showed a significant decrease in tumour uptake, and the $^{18}$F-FDG uptake did not change. In A549 tumours, the tumour volume appeared to increase over time ; therefore, the tumour suppressive effect of irradiation may have been temporary. Our data suggested that cells with a more aggressive phenotype may have led to regrowth after irradiation, which affected $^{18}$F-FDG uptake 1 week after irradiation. When using $^{18}$F-FDG in radiotherapy, the effect of radiation-induced inflammation should be considered because this inflammation causes an increase in glucose uptake. The inflammatory reaction is substantial approximately 1 month after radiation treatment, and the earliest evaluation of therapeutic effectiveness is recommended at 6–8 weeks after irradiation (25). Therefore, there have been few studies of the effect of inflammation on $^{18}$F-FDG uptake at an early stage, within 1 month after irradiation, regardless of whether it is normal or tumour tissue. In this study, pathological analyses revealed neutrophil infiltration at the margins of the necrotic tumour lesions, and the possibility that $^{18}$F-FDG uptake was caused by acute radiation-induced inflammation 1 week after irradiation could not be disregarded. However, similar pathological findings were obtained in FT821 tumours, which demonstrated radiation-mediated antitumour effects without an increase in $^{18}$F-FDG accumulation. Therefore, the effect of radiation-induced acute inflammation on $^{18}$F-FDG accumulation was considered to be small.

$^{18}$F-FLT is expected to contribute to individual therapy because this method accurately evaluates the decrease in tumour activity that cannot be captured by $^{18}$F-FDG. However, $^{18}$F-FLT cannot assess the presence or absence of surviving tumour cells and is merely an indicator of proliferative activity. Everitt *et al*. suggested that $^{18}$F-FLT appears to be a more sensitive tracer of early treatment responses than $^{18}$F-FDG, although it is currently unclear whether these changes predict eventual clinical outcomes (19), and our study supports this proposal. Furthermore, $^{18}$F-FDG may be useful for evaluating surviving cells without being affected by the inflammatory reaction at an extremely early stage, approximately 1 week after irradiation. The combined use of $^{18}$F-FLT and $^{18}$F-FDG makes it possible to accurately predict the effects of radiotherapy, which may lead to minimally invasive personalised therapy.

Our evaluation of $^{18}$F-FDG accumulation during the radiation-associated inflammatory response had several limitations. Because of the laws pertaining to the use of radioisotopes and the regulations of the facility, PET evaluations before and after irradiation on the same individual were not possible. To match the experimental conditions, data were all obtained from model mice using cell lines that were cultured and transplanted with the same timing. However, evaluation in the same individual will eliminate unnecessary bias and provide more reliable results. The relationship between $^{18}$F-FDG accumulation and radioactive inflammation is an important factor and the degree of radioactive inflammation was evaluated by changes in neutrophil counts by haematoxylin and eosin staining in this study. Furthermore, the evaluation period was only 1 week after irradiation. Assessing data over a longer duration using immunohistochemical staining might be useful for evaluating inflammation more objectively with more reproducible results.

## CONCLUSION

To predict the therapeutic effect of irradiation using PET imaging, tumour cell proliferative activity and cell death need to be clearly separated. We demonstrated some of the limitations and further possibilities of using $^{18}$F-FLT and/or $^{18}$F-FDG PET/CT to evaluate radiotherapeutic efficacy in mouse models of NSCLC. These findings may have implications for clinical tumour responses after radiotherapy in humans.

## CONFLICTS OF INTERESTS AND SOURCE OF FUNDING

This work was supported in part by the Japan Society for the Promotion of Science (JSPS) Grants-in-Aid for Scientific Research (KAKENHI), grant No. 20K07698. The authors declare that they have no conflicts of interest.

## ACKNOWLEDGEMENTS

We thank Dr Haruhiko Fujino (Tokushima University, Tokushima, Japan) who established the FT821 cell line using a primary culture from surgically resected tissue. We thank Susan Zunino, PhD, and J. Ludovic Croxford, PhD, from Edanz (https://jp.edanz.com/ac) for editing a draft of this manuscript.

## REFERENCES

1. Thomas M, Macha HN, Ukena D, Hamm M, Deppermann M, Semik M, Riesenbeck D, Rübe C, Heinecke A : Cisplatin/etoposide (PE) followed by twice-daily chemoradiation (hfRT/CT) versus PE alone before surgery in stage III non-small cell lung cancer (NSCLC) : a randomised phase III trial of the German Lung Cancer Cooperative Group (GLCCG). J Clin Oncol 22 : 7004, 2004
2. Faber LP, Kittle CF, Warren WH, Bonomi PD, Taylor 4th SG, Reddy S, Lee MS : Preoperative chemotherapy and irradiation for stage III non-small cell lung cancer. Ann Thorac Surg 47 : 669-75 ; discussion 676-7, 1989
3. Skarin A, Jochelson M, Sheldon T, Malcolm A, Oliynyk P, Overholt R, Hunt M, Frei 3rd E : Neoadjuvant chemotherapy in marginally resectable stage III M0 non-small cell lung cancer : Long-term follow-up in 41 patients. J Surg Oncol 40 : 266-74, 1989
4. Okawara G, Mackay JA, Evans WK, Ung YC : Management of unresected stage III non-small cell lung cancer : a systematic review. J Thorac Oncol 1 : 377-93, 2006
5. Albain KS, Scott CB, Rusch VR, Turrisi AT, Shepherd FA, Smith C, Gandara DR, Johnson DH, Green MR, Miller RC, for RTOG, SWOG, NCIC-CTG, ECOG, CALGB : NCCTG Phase III comparison of concurrent chemotherapy plus radiotherapy (CT/RT) and CT/RT followed by surgical resection for stage IIIA (pN2) non-small cell lung cancer : initial results from intergroup trial 0139 (RTOG 93-09). Proc Am Soc Clin Oncol 22 : 621, 2003
6. Christensen JD, Colby TV, Patz Jr EF : Correlation of [18F]-2-fluoro-deoxy-D-glucose positron emission tomography standard uptake values with the cellular composition of stage I nonsmall cell lung cancer. Cancer 116 : 4095-102, 2010
7. Sauter AW, Spira D, Schulze M, Pfannenberg C, Hetzel J, Reimold M, Klotz E, Claussen CD, Horger MS : Correlation between [$^{18}$F]FDG PET/CT and volume perfusion

CT in primary tumours and mediastinal lymph nodes of non-small-cell lung cancer. Eur J Nucl Med Mol Imaging 40 : 677-84, 2013
8. Mac Manus MP, Hicks RJ, Matthews JP, Wirth A, Rischin D, Ball DL : Metabolic (FDG-PET) response after radical radiotherapy/chemoradiotherapy for non-small cell lung cancer correlates with patterns of failure. Lung Cancer 49 : 95-108, 2005
9. Hicks RJ, Mac Manus MP, Matthews JP, Hogg A, Binns D, Rischin D, Ball DL, Peters LJ : Early FDG-PET imaging after radical radiotherapy for non-small-cell lung cancer : inflammatory changes in normal tissues correlate with tumour response and do not confound therapeutic response evaluation. Int J Radiat Oncol Biol Phys 60 : 412-8, 2004
10. Zheng Y, Yang Z, Zhang Y, Shi Q, Bao X, Zhang J, Yuan H, Yao Z, Hu C, Zhang Y : The preliminary study of 18F-FLT micro-PET/CT in predicting radiosensitivity of human nasopharyngeal carcinoma xenografts. Ann Nucl Med 29 : 29-36, 2015
11. Chalkidou A, Landau DB, Odell EW, Cornelius VR, O'Doherty MJ, Marsden PK : Correlation between Ki-67 immunohistochemistry and 18F-fluorothymidine uptake in patients with cancer : a systematic review and meta-analysis. Eur J Cancer 48 : 3499-513, 2012
12. Fujino H, Kondo K, Miyoshi T, Ishikura H, Takahashi Y, Sawada N, Hirose Y, Takizawa H, Nagao T, Sakiyama S, Monden Y : Establishment of patient-like SCID mouse model by orthotopically implanting primary cultured cells from surgically-resected lung cancer tissues. Oncol Rep 10 : 1709-15, 2003
13. Otani T, Kondo K, Takizawa H, Kajiura K, Fujino H, Otsuka H, Miyoshi H : Non-invasive monitoring of cisplatin and erlotinib efficacy against lung cancer in orthotopic SCID mouse models by small animal FDG-PET/CT and CT. Oncol Rep 41 : 447-54, 2019
14. Kitao T, Hirata K, Shima K, Hayashi T, Sekizawa M, Takei T, Ichimura W, Harada M, Kondo K, Tamaki N : Reproducibility and uptake time dependency of volume-based parameters on FDG-PET for lung cancer. BMC Cancer 16 : 576, 2016
15. Hoshikawa H, Mori T, Yamamoto Y, Kishino T, Fukumura T, Samukawa Y, Mori N, Nishiyama Y : Prognostic value comparison between 18F-FLT PET/CT and 18F-FDG PET/CT volume-based metabolic parameters in patients with head and neck cancer. Clin Nucl Med 40(6) : 464-8, 2015
16. Lloyd R, Osamura RY, Kloppel G, Rosai J : WHO classification of tumours of endocrine organs. 4th ed. Lyon : IARC Press : 2017
17. Magota K, Kubo N, Kuge Y, Nishijima K, Zhao S, Tamaki N : Performance characterization of the Inveon preclinical small-animal PET/SPECT/CT system for multimodality imaging. Eur J Nucl Med Mol Imaging 38 : 742-52, 2011
18. Molthoff CF, Klabbers BM, Berkhof J, Felten JT, van Gelder M, Windhorst AD, Slotman BJ, Lammertsma AA: Monitoring response to radiotherapy in human squamous cell cancer bearing nude mice : comparison of 2'-deoxy-2'-[$^{18}$F] fluoro-D-glucose (FDG) and 3'-[$^{18}$F]fluoro-3'-deoxythymidine (FLT). Mol Imaging Biol 9 : 340-7, 2007
19. Everitt SJ, Ball DL, Hicks RJ, Callahan J, Plumridge N, Collins M, Herschtal A, Binns D, Kron T, Schneider M, MacManus M : Differential $^{18}$F-FDG and $^{18}$F-FLT uptake on serial PET/CT imaging before and during definitive chemoradiation for non-small cell lung cancer. J Nucl Med 55(7) : 1069-74, 2014
20. Christensen TN, Langer SW, Persson G, Larsen KR, Loft A, Amtoft AG, Berthelsen AK, Johannesen HH, Keller SH, Kjaer A, Fischer BM : $^{18}$F-FLT PET/CT adds value to $^{18}$F-FDG PET/CT for diagnosing relapse after definitive radiotherapy in patients with lung cancer : results of a prospective clinical trial. J Nucl Med 62 : 628-35, 2021
21. Buck AK, Halter G, Schirrmeister H, Kotzerke J, Wurziger I, Glatting G, Mattfeldt T, Neumaier B, Reske SN, Hetzel M : Imaging proliferation in lung tumors with PET : $^{18}$F-FLT versus $^{18}$F-FDG. J Nucl Med 44 : 1426-31, 2003
22. Gerbaudo VH, Killoran JH, Kim CK, Hornick JL, Nowak JA, Enzinger PC, Mamon HJ : Pilot study of serial FLT and FDG-PET/CT imaging to monitor response to neoadjuvant chemoradiotherapy of esophageal adenocarcinoma : correlation with histopathologic response. Ann Nucl Med 32 : 165-74, 2018
23. Wang Z, Wang Y, Sui X, Zhang W, Shi R, Zhang Y, Dang Y, Qiao Z, Zhang B, Song W, Jiang J : Performance of FLT-PET for pulmonary lesion diagnosis compared with traditional FDG-PET : a meta-analysis. Eur J Radiol 84 : 1371-7, 2015
24. Jensen MM, Kjaer A : Monitoring of anti-cancer treatment with $^{18}$F-FDG and $^{18}$F-FLT PET : a comprehensive review of pre-clinical studies. Am J Nucl Med Mol Imaging 5(5) : 431-56, 2015
25. Goerres GW, Schmid DT, Bandhauer F, Huguenin PU, von Schulthess GK, Schmid S, Stoeckli SJ : Positron emission tomography in the early follow-up of advanced head and neck cancer. Arch Otolaryngol Head Neck Surg 130 : 105-9, 2004. doi : 10.1001/archotol.130.1.105.